Catalysis Communications 185 (2023) 106800

Contents lists available at ScienceDirect

Catalysis Communications

journal homepage: www.elsevier.com/locate/catcom

Ni alumina-based catalyst for sorption enhanced reforming - Effect of calcination temperature

Lj. Gavrilović [a,*], S.S. Kazi [a], A. Nelson [a,b], A.G.P. Oliveira [a], J. Meyer [a]

[a] Institute for Energy Technology, Instituttveien 18, Kjeller 2007, Norway
[b] ZEG POWER AS, Postboks 102, Kjeller 2027, Norway

ARTICLE INFO

Keywords:
Sorption enhanced reforming
Ni catalyst
Hydrogen
Stability

ABSTRACT

Effect of calcination temperature (350 °C – 850 °C) on the physicochemical properties as well as catalytic performance of Ni-based catalyst for the hydrogen production via steam methane reforming (SMR) and sorption enhanced reforming (SER) has been investigated. Catalyst calcined at highest temperature (850 °C) shows formation of $NiAl_2O_4$ confirmed by XRD. Consequently, a much higher reduction temperature (875 °C) is required to reduce this Ni aluminate spinel to an active Ni catalyst. Catalyst calcined at highest temperature (850 °C) showed much higher CH_4 conversion and H_2 production in SMR compared to the catalysts calcined at lower temperatures. In addition, higher CH_4 conversion and H_2 production was observed for the 15%Ni/alumina_850 catalyst after aging (long exposure to steam and high temperature) compared to commercial reforming catalyst. Finally, a much better stability is observed for the 15%Ni/alumina_850 catalyst compared to the commercial reforming catalyst after 100 SER/regeneration cycles under relevant reaction conditions. The formation of $NiAl_2O_4$ during high temperature calcination plays a vital role in the robustness and stability of the Ni-based catalysts and can be useful synthesis procedure for increasing the catalyst lifetime.

1. Introduction

The International Energy Agency's "Net Zero by 2050" report [1] is the world's first comprehensive roadmap for the global energy sector to reach net-zero emissions by 2050. A vital message in this report is that clean hydrogen is a central pillar to reach a net-zero state. Clean hydrogen produced from natural gas with CO_2 capture will be key to supply increasing demand to an acceptable cost. In addition, the oil and gas sector already consume a significant and increasing amount of hydrogen and it is expected that this sector will rely on clean hydrogen for many years to come. Because Carbon Capture and Storage becomes a requirement, clean hydrogen technologies will need to minimize capital and operational costs to stay competitive compared to alternatives. Sorption-Enhanced Reforming (SER) process can greatly contribute to achieving these goals. SER is an alternative reforming process to the conventional steam reforming of methane [2,3]. The SER process involves using a high-temperature CaO-based solid CO_2 sorbent and a reforming catalyst. In the process, reforming, water-gas shift (WGS), and CO_2 capture (carbonation) co-occur. The process is based on Le Chatelier's principle, which, due to the simultaneous in-situ CO_2 capture by sorbent, results in shifting the thermodynamic equilibrium towards hydrogen production, thus enhancing the hydrogen yield [4]. The main advantages of the SER process compared to a conventional reforming process are: 1) fewer reaction vessels are needed 2) higher hydrogen yields (>95 mol%, dry basis) per one single process step 3) no need for WGS catalysts, and 4) improved energy efficiency due to the integration of heat between the exothermic carbonation and endothermic reforming reaction. This consequently brings significant capital cost savings, and footprint reduction.

CaO-based CO_2 sorbents, such as calcined limestone (CaO) and dolomite (mixed Ca—Mg oxides) are available in nature and have high theoretical CO_2 sorption capacity (79 g_{CO2}/100 g_{CaO}) and fast capture kinetics in the temperature range of 600–700 °C and ambient pressure [5]. However, the sorption capacity of natural sorbents declines rapidly in the multi-cycle carbonation-calcination process due to pore blockage and sintering [6], resulting in a residual CaO conversion below 10% (< $8gCO_2$/100gCaO) after a few hundred cycles [7]. To overcome these, extensive research work has been conducted in our lab towards the development of synthetic sorbent consisting of sub-microparticles of CaO (~100 nm) distributed in micro-porous mayenite support ($Ca_{12}Al_{14}O_{33}$) which showed a promising stable CO_2 capture capacity (21 g-CO_2/100 g sorbent) under severe calcination conditions and have

* Corresponding author.
E-mail address: ljubisa.gavrilovic@ife.no (Lj. Gavrilović).

https://doi.org/10.1016/j.catcom.2023.106800
Received 25 July 2023; Received in revised form 16 October 2023; Accepted 12 November 2023
Available online 15 November 2023

high mechanical strength compared to natural CO_2 sorbents [8,9]. This synthetic sorbent is used in the present work for the SER experiments.

As mentioned above the SER process involves a high-temperature CaO-based solid CO_2 sorbent and a reforming catalyst. There is no commercial catalyst dedicated to SER processes, but typical SMR industrial catalysts that can be used are Ni and Fe [10]. While Fe is an attractive choice due to its price and availability, Ni is the preferred catalyst due to its high activity and hydrogen selectivity. The common SER catalysts reported in the literature are promoted Ni-based catalyst mostly supported in alumina [11–14]. The SER process has been successfully validated in our laboratory-scale reactors with CaO-based sorbents and a commercial Ni-based catalyst in fluidized bed systems [8]. Although the chosen commercial reforming catalyst shows good mechanical properties, the catalysts suffer from long-term deactivation when exposed to SER multi-cycling process conditions. In other words, the regeneration atmosphere is rather different than the commercial catalysts are designed for, i.e., there are significant amounts of steam, low to zero hydrogen and some oxygen in the case of an oxy-fuel regenerator. The presence of a high concentration of steam at a high temperature (850 °C), with low or no presence of hydrogen, leads to Ni-migration and sintering effects [15]. The presence of oxygen leads to partial oxidation of the catalyst, and consequently, the material is exposed to reduction-oxidation cycles, which also leads to sintering. One option for reducing the effect of regeneration gas atmosphere on catalyst performance is to add a small amount of H_2 during regeneration [16]. Furthermore, a high thermodynamic potential for coke formation during reforming reaction can occur [17], thus covering the Ni surface or leading to the formation of carbon nanotubes, which will eventually lift the Ni particle from the support surface and thereby break the anchoring bonds between Ni and the support. All above mentioned mechanisms are sources of catalytic deactivation [18]. It has been reported that Ni alumina catalyst calcined at higher temperature during synthesis leads to the formation of Ni aluminate spinel [19–23] which gives more robust catalyst resistant towards deactivation. This has also been confirmed in the dry reforming of methane [24], steam reforming of ethanol [25,26], reforming of bio-oil [27,28], steam reforming of liquefied natural gas [29], but there has not been study on the sorption enhanced reforming (SER). Therefore, the aim of the present paper is to develop a reforming catalyst tailored for SER process -and its multiple reforming-regeneration cycles to provide high H_2 yield with higher catalyst stability.

2. Experimental

2.1. Material synthesis

2.1.1. Catalyst synthesis

A 15% Ni alumina-based catalyst was synthesized using incipient wetness impregnation (IWI) method. The as received alumina support (Sasol) was calcined at 850 °C for 1 h before impregnating with nickel precursor ($Ni(NO_3)_2 \cdot 6H_2O$, Acros Organics). Isopropanol (IPA) was used as a solvent. A 3-steps IWI impregnation was needed to synthesize 15wt%Ni-based catalyst using IPA since Ni-nitrate is less soluble in IPA, and IPA evaporates at room temperature. The volume of the Ni-nitrate solution added corresponds to the pore volume of the alumina support. The Ni-nitrate solution was added to the alumina support surface drop-by-drop and mixed afterwards until homogeneous. Capillary action draws the Ni- nitrate solution into the pores of the alumina support. The impregnated catalysts were dried and calcined at a different temperature (350 °C - 850 °C) in presence of air (heating rate, 278 K/min).

2.1.2. Sorbent synthesis

Mayenite ($Ca_{12}Al_{14}O_{33}$) supported CaO based sorbent was prepared by hydrothermal synthesis. Calcium hydroxide ($Ca(OH)_2$, Alfa Aesar) and aluminum hydroxide ($Al(OH)_3$, Merck) were used as precursors and water as solvent. Stoichiometric amounts of the precursors were weighed and transferred to the stainless-steel autoclave and mixed to produce a homogeneous mixture. Deionized water was added at a liquid-to-solid weight ratio, L/S equal to 3. The slurry was heated up, under mixing at 120 °C for 3 h, resulting in a pressure increase up to 2–3 bars in the autoclave. After hydrothermal synthesis, the product slurry from the autoclave was collected at room temperature and evaporated in a drying oven at 110 °C overnight. At that stage a hydrogarnet powder ($Ca_3Al_2(OH)_{12}$) with excess of $Ca(OH)_2$ was obtained. Finally, to obtain final composition of the sorbent powder, the dried hydrogarnet containing sorbent powder was thermally treated in a furnace at 1000 °C in air for 1 h (heating rate, 5 °C/min). This sorbent was used in the sorption-enhanced reforming test. The characterization and testing (carbonation/calcination) of the sorbent is not part of this study and those results can be found in our previous publications [9,30].

2.2. Catalyst characterization

2.2.1. X-ray diffraction (XRD)

XRD was employed to identify the phases present in fresh calcined, reduced and spent catalysts using a Bruker D2 phaser diffractometer with Cu Kα radiation (30 kV and 10 mA). Patterns were recorded from 10 to 90° (2θ) in 0.02 steps. The EVA software was used for phase identification with the PDF-42017 database. Rietveld refinements were performed with the TOPAS software for quantitative phase analysis and Ni crystallite size estimation.

2.2.2. Brunauer–Emmett–Teller (BET)

The pore volume, pore size and pore diameter of the catalysts were measured using a 3-Flex analyzer (Micromeritics). The catalysts were degassed at 300 °C under vacuum overnight before surface measurements. The catalyst surface properties were determined by N_2 physisorption at a temperature of −196 °C (77 K).

2.2.3. Temperature programmed reduction (H_2-TPR)

Temperature programmed H_2 reduction (H_2-TPR) was carried out using a 3-Flex analyzer (Micromeritics). The reduction behavior and interaction between the active phase and each catalyst support were studied using H_2-TPR. Before H_2-TPR, TPD was performed on catalysts to remove any adsorbed water in the sample. The catalyst (100–200 mg) was loaded into a U-type quartz microreactor and heated in N_2 from room temperature to 600 °C at the rate of 283 K/min, followed by cooling in N_2. In the TPR experiment, the pre-treated catalyst sample was then treated in 100 vol% N_2 flow (10 mln/min) at room temperature for about 15 min until the baseline was stabilized. The reduction was carried out from the ambient temperature to 900 °C with a heating rate of 283 K/min in a flow of 10/90 vol% H_2/N_2 (50 mln/min) for 30 min. Any reaction products, e.g., water generated during TPR was trapped in a cooling chamber (located between the reactor and TCD) containing a freezing mixture (ice with salt, T: -15 °C). After TPR, the sample was cooled down to ambient temperature under N_2 flow. A thermal conductivity detector (TCD) determines quantitively the consumption of hydrogen.

2.2.4. H_2-Pulse chemisorption

A pulse chemisorption was carried out using a 3-Flex analyzer (Micromeritics) to determine Ni dispersion and Ni particle size. The injected gas (100% H_2) chemisorbs on Ni active site until all active sites have reacted. The first few injections may be consumed, and no change in signal from the TCD detector is recorded. As the sample approaches saturation, peaks representing concentrations of unreacted molecules appear. After the reaction has completed, each of the discretely injected gas (H_2) volumes emerge from the sample unchanged, and the detected peaks are constant in area. The quantity of molecules chemisorbed is the difference between the total amount of reactant gas injected and the sum amount that did not react with the sample's active sites as measured by the TCD detector.

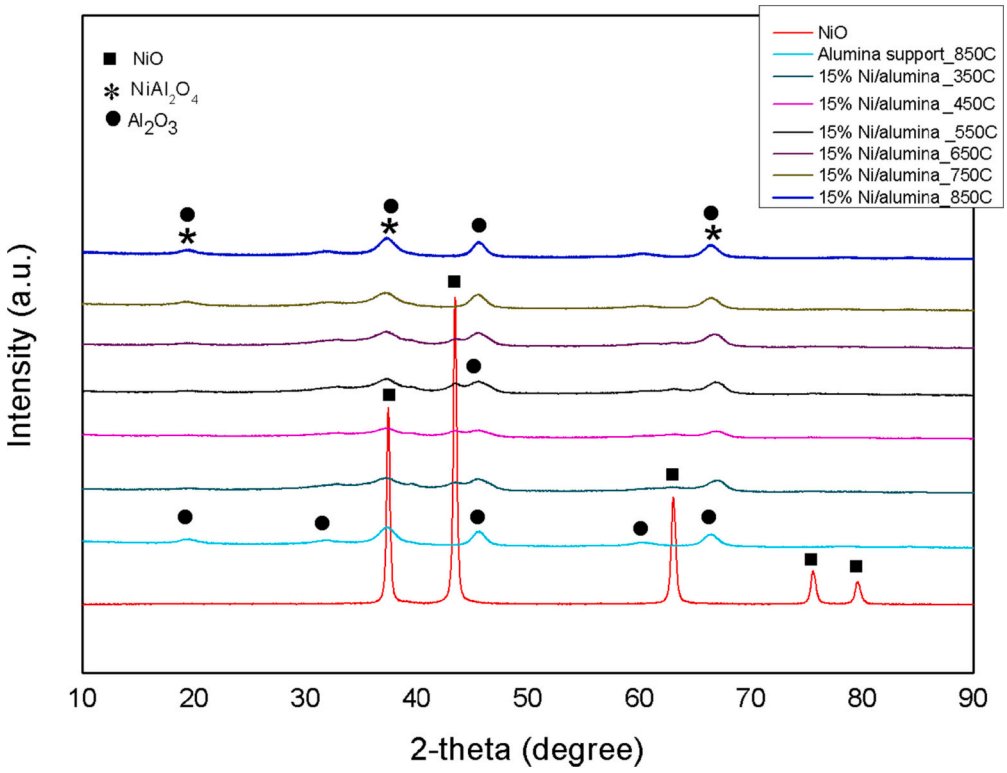

Fig. 1. XRD patterns for the catalysts calcined at different temperatures.

2.3. Catalyst testing

2.3.1. Steam methane reforming

Steam methane reforming (SMR) was performed in the quartz packed bed reactor (50 mm length and 12 mm external diameter). The PBR was filled with a solid mixture of 50 mg catalyst together with 500 mg of crushed quartz (355–1000 μm). The catalysts reduction was performed in 10/90 vol% H_2/N_2 for 1 h at 650–875 °C depending on the calcination temperature of the synthesized catalysts. After reduction, sample was cooled down to the reaction temperature (650 °C) in 10/90 vol% H_2/N_2 mixture. The SMR reaction was performed at three different gas space velocity (GSV) of 30, 63 and 123 g-CH_4 /h g-catalyst by flowing methane and steam. The system was held for 10 min to reach the steady state before switching to another GSV. The product gas was analyzed by the gas analyzer SICK GMS840. Calculated missing carbon was negligible in these experiments.

Furthermore, the catalytic performance of the commercial (15%Ni) and 15%Ni/alumina_850 was studied after aging i.e., exposing the catalyst to the harsh regeneration environment. The PBR reactor was filled with the 300 mg of catalyst. The commercial catalyst is received in a reduced state. The 15%Ni/alumina_850 catalyst was reduced by flowing 10/90 vol% H_2/N_2 at 875 °C (heating rate, 10 °C/min). The reactor was then cooled down to 650 °C in 10/90 vol% H_2/N_2. The catalysts were first tested in the SMR conditions at GSV of 5.4 g-CH_4 /h g-catalyst flowing methane and steam before exposing it to the 67 h of regeneration conditions (850 °C, 42.1/31.6/5,3/21.1 vol% $CO_2/H_2O/H_2/N_2$). The catalysts were then tested under the same SMR conditions at the beginning of the experiment to compare the catalytic activity.

2.3.2. Sorption-enhanced reforming

Sorption-enhanced reforming was performed in-house built Thermogravimetric analyzer (TGA, CI electronics) to assess catalyst performance after 100 SER/regeneration cycles. Typically, 27.3 mg of material (sorbent-to reduced catalyst weight ratio of 3) were loaded in an Al_2O_3 non-porous crucible (8 mm ID, 10 mm height) in 100 vol% N_2 flowing downwards through the reactor. Prior to SER test, in-house prepared Ni catalysts were pre-reduced separately at 875 °C in a gas mixture, 50/50 vol% H_2/N_2 (F_{total}: 500 mln/min) for 1 h. Commercial catalyst was supplied in reduced (Ni) state. In all cases, the reforming was performed at 600 °C using steam to methane volume ratio of 4 under a gas mixture of 14/43/43 vol% $CH_4/ H_2O/N_2$ (F_{total}: 875 mln/min) for 35 min. After reforming, the gas composition was then switched to 29/68/3 vol% $H_2O/N_2/H_2$ and temperature was raised to perform regeneration at 850 °C for 8 min. This small amount of H_2 (3 vol%) was added to prevent re-oxidation of the Ni catalyst. Multi-cycles consisting of reforming and regeneration steps were repeated up to 100 cycles to determine the long-term behavior of the catalyst.

3. Results

The following chapters present the influence of calcination temperature on catalyst particle size, reducibility, morphological characteristics as well as its effect on CH_4 conversion, H_2 production and stability in SMR. Moreover, the comparison between catalyst activity and stability in SER of the commercial catalyst and the catalyst calcined at 850 °C i.e., 15%Ni/alumina_850 is discussed.

3.1. Characterization results

3.1.1. Catalysts crystalline structure

After catalyst synthesis, treatment at high calcination temperature, Ni^{2+} could disperse on the surface of Al_2O_3 or diffuse into the bulk structure of Al_2O_3 to various extents to form nickel aluminate [31]. Therefore, the synthesized catalyst usually constitutes a mixture of two nickel phases, namely nickel oxide (NiO) and nickel aluminate ($NiAl_2O_4$). This is confirmed by XRD patterns of the catalyst treated at 6 different calcination temperatures (350, 450, 550, 650, 750 and 850 °C), Fig. 1. NiO peaks appear at 2θ ~ 37.2, 43.2, 62.8, 75.3 and 79.4 respectively, confirmed from XRD of NiO standard sample. The samples calcined at 350 °C and 450 °C show less sharp NiO peaks, whereas

Table 1
Effect of calcination temperature on NiO/Ni crystalline size.

Catalyst	Calcination temperature (°C)	NiO crystallite size (nm)	Ni crystallite size (nm)
15%Ni/ alumina	350	3.3	–
	450	4.5	–
	550	4.6	11.5
	650	4.5	–
	750	–	–
	850	–	17.0

Table 2
Morphological characteristics of the support and the catalysts.

Material	Calcination temperature (°C)	BET		
		Surface area (m^2/g)	Pore volume (cm^3/g)	Average pore diameter (nm)
Alumina support	850	175	0.5	15.2
15%Ni/ alumina catalyst	350	134	0.34	10.3
	450	132	0.36	10.9
	550	129	0.36	11.2
	650	125	0.35	11.0
	750	125	0.36	11.6
	850	121	0.36	11.8

samples treated at 550 °C exhibit a sharper NiO peak which confirms high crystallinity of NiO. The samples calcined at higher temperatures (750 and 850 °C) exhibit shifting of the Al_2O_3 peaks (2Θ = 19°, 38° and 67°) to a lower angle which indicates the formation of $NiAl_2O_4$ [31,32]. Table 1 summarizes the NiO crystallite size of the 15%Ni/alumina catalysts after calcination at different temperatures. The NiO crystallite size slightly increased while increasing the calcination temperature from 350 °C to 450 °C. However, it does not show any significant change in crystallite size on further increasing calcination temperature up to 650 °C. The NiO crystallite size was impossible to detect for those calcined above 750 °C due to the formation of $NiAl_2O_4$. However, some bulk NiO might be present together with $NiAl_2O_4$ phases. The Table 1 also shows the Ni crystallite size for the reduced 15%Ni/alumina_550 and 15%Ni/alumina_850 catalysts since these two were used in the further testing in the next chapters. The same trend is observed here, the catalyst calcined at higher temperature exhibit larger Ni crystallite size.

3.1.2. Catalyst morphological characteristics

The effect of the calcination temperature on the catalyst morphological characteristics is shown in Table 2. The catalysts specific surface area decreased with increasing the calcination temperature while the pore volume and average pore diameter remained the same. Catalyst calcined at 350 °C has the highest surface area of 133.6 m^2/g, while the catalyst calcined at 850 °C has the lowest surface area of 120.8 m^2/g. The reduction of the surface area, pore volume and average pore diameter of the catalyst compared to the pure alumina is attributed due to the closing of pores of the support by the active Ni phase. However, increase in pore diameter with increasing calcination temperature (350–850 °C) is also observed. This might be due to the collapse of smaller pores and formation of larger pores at higher calcination temperature [33].

3.1.3. Catalyst reduction profiles

The effect of calcination temperatures on the TPR profiles of the 15% Ni/alumina catalysts is presented in Fig. 2. Reduction peaks of the catalysts calcined at higher temperature are shifted towards higher temperatures. It means that much higher temperature is required to reduce those catalysts. The maximum reduction temperature, T^{max} for the samples calcined at 350 °C, 450 °C, 550 °C, 650 °C, 750 °C and 850 °C is 536 °C, 570 °C, 660 °C, 726 °C, 824 °C and 900 °C, respectively. TPR peak at 245 °C for 15%Ni/alumina_350 catalyst corresponds to the presence of residual nitrates (from the precursor) after calcination. Broad peaks and shoulders are observed for the low temperature calcined catalysts. This is due to the presence non-stoichiometric NiO and different types of NiO (α or β) formed on the support [34]. A broad TPR peak for the catalyst calcined up to 650 °C might also be due to the reduction of bulk NiO species and weak interactions with the support. Catalysts calcined at a higher temperature (750 °C and 850 °C) exhibit a sharp single TPR peak which probably corresponds to the reduction of formed $NiAl_2O_4$ [32] during high temperature calcination. This correlates well with the XRD profiles (Fig. 1) indicating that increasing

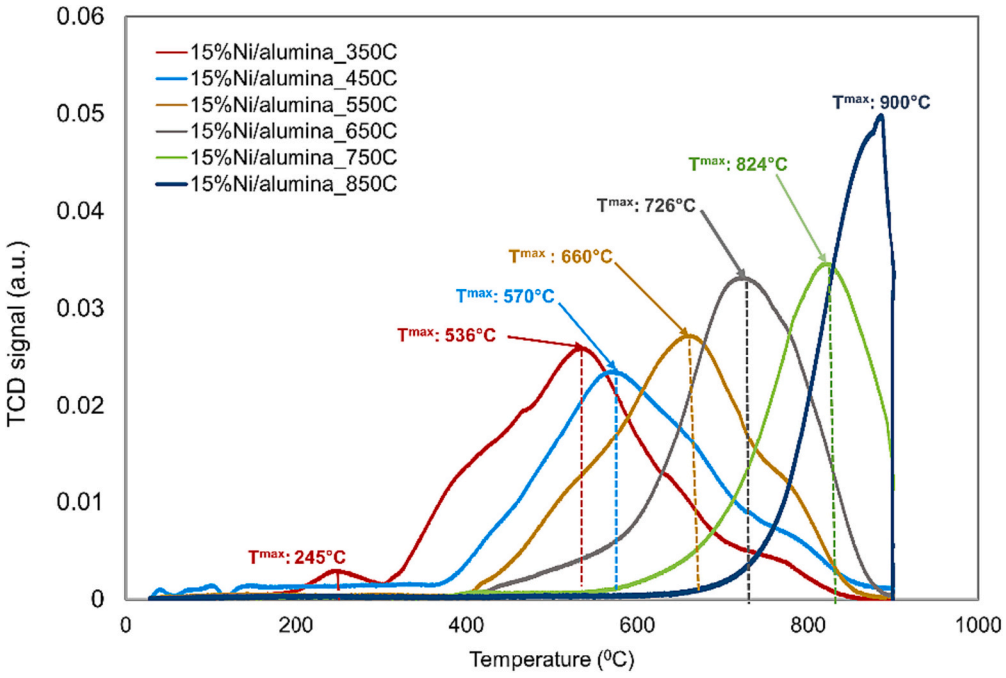

Fig. 2. TPR profiles of 15%Ni/alumina catalyst calcined at different temperatures.

Table 3
Influence of temperature on Ni dispersion.

Catalyst	Calcination temperature (°C)	Reduction temperature (°C)	Ni Dispersion (%)
15%Ni/ alumina	350	600	4.8
	450	600	3.9
	550	670	2.3
	850	850	2.5

calcination temperature enhances metal-support (Ni-Al_2O_3) interaction and leads to the formation of strong $NiAl_2O_4$ phase [19,35].

3.1.4. Ni dispersion

The effect of calcination temperature on Ni dispersion was investigated using H_2 pulse chemisorption and is summarized in Table 3. The reduction temperatures were selected based on the TPR profiles. The Ni dispersion decreases with increasing the calcination temperature. This decrease in Ni dispersion can be attributed to the strong metal oxide support interaction and the decrease in the availability of surface nickel oxide atoms [23]. In addition, by increasing the calcination temperature diffusion of active metal into bulk catalyst support is reported [21].

3.2. Activity results

3.2.1. SMR - Influence of calcination temperature and GSV

The influence of calcination temperature as well gas space velocity (GSV) on CH_4 conversion and H_2 yield on 15%Ni/alumina catalysts as well as commercial one was investigated. It is important to mention here that the GSV is set to much higher values to stress the catalyst to its maximum activity. All the tested catalyst samples show a decrease in CH_4 conversion and H_2 production with increasing the (GSV), Fig. 3. The catalyst calcined at 850 °C shows higher CH_4 conversion and higher H_2 concentration for all GSV compared to the catalysts calcined at lower temperatures. Similar methane conversions and H_2 production were observed for the catalyst calcined at 850 °C and commercial catalyst for the two GSV investigated. However, for the highest GSV, the commercial catalyst showed lower conversion compared to the 15%Ni/alumina_850 catalyst. This suggests that formation of $NiAl_2O_4$ (non-active phase for the SMR), which after reduction, provides a more active and a robust catalyst [20].

3.2.2. SMR – effect of aging

For further testing and comparison with the commercial catalyst we have selected 15%Ni/alumina_850 sample since it showed the best catalytic performance in the above SMR tests. To assess the catalyst stability, the performance of the commercial and 15%Ni/alumina_850 catalysts has been compared before and after aging, Table 4. Fresh 15% Ni/alumina_850 shows slightly higher CH_4 conversion (98%) compared to the commercial one (96%). However, after being exposed to the regeneration conditions for 67 h, 15%Ni/alumina_850 shows almost the same CH_4 conversion (96%) while CH_4 conversion of the commercial catalyst reduced to 91%. This indicates that the catalyst calcined at high calcination temperature is more robust, showing better catalytic activity and stability. This is further confirmed by measuring Ni crystallite size of the aged catalysts and compared with the fresh ones. The Ni crystallite size of the fresh commercial and 15%Ni/alumina_850 is 15 nm and 17 nm, respectively. After aging the growth of Ni crystallite size is observed for both catalysts. However, crystallite size growth is more pronounced in case of commercial catalyst (15 nm to 43.1 nm) compared to 15%Ni/alumina_850 (17 nm to 33 nm) catalyst.

It is reported that this strong interaction between Ni and Al_2O_3 plays a vital role in the stability of Ni catalyst [36]. The formation of $NiAl_2O_4$ spinel has generally been considered for the deactivation of Ni/Al_2O_3 catalysts during CH_4 reforming [10,37]. However, the inactive $NiAl_2O_4$ spinel plays an important role for the reforming catalyst [38]. It is speculated that the active Ni sites are present in a monodisperse form on the special sites of the $NiAl_2O_4$ structure [39]. Increase in calcination temperature may result in the partial diffusion of NiO into the Al_2O_3 support which prevents the migration of Ni particles as well as anchoring of Ni particles on the support, thus preventing sintering [21].

3.2.3. SER – effect of cyclic operation

To further elucidate the stability of the 15%Ni/alumina_850 catalyst, the catalyst was studied in Sorption-enhanced reforming reaction in TGA where 100 reforming/regeneration cycles were performed. In addition, the commercial catalyst was tested as a reference catalyst and results were compared. The same sorbent was used in both experiments. It is not possible to connect the effluent gas stream from the TGA to the gas analyzer in the current set-up which means we are not able to calculate methane conversion and H_2 production. However, if the catalyst is active, the produced CO_2 will be captured by sorbent and the

Table 4
CH_4 conversion of fresh and aged catalysts.

Catalyst	CH_4 conversion (g-CH_4/g-catalyst)	
	fresh	aged
15%Ni/Al_2O_3_850	97.7	96.2
Commercial	96	91.3

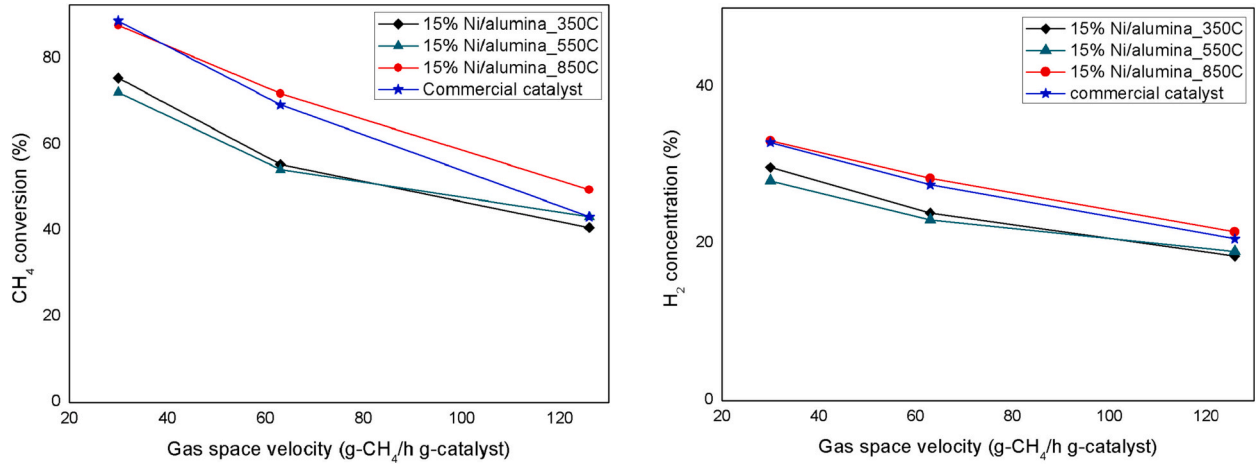

Fig. 3. Effect of calcination temperature on CH_4 conversion (left) and H_2 concentration (right) at different GSV for 15%Ni/alumina and comparison with commercial catalyst. Reforming: T: 650 °C, 44.6/32.5/22.9 vol% $CH_4/H_2O/N_2$ at different GSV.

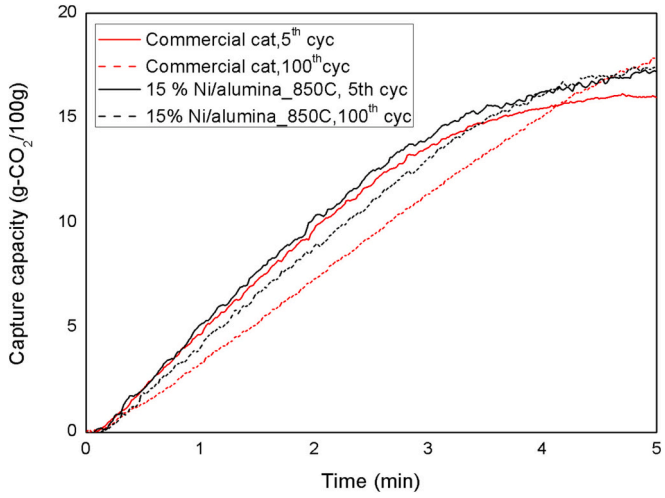

Fig. 4. Comparison of catalytic activity of the commercial and 15% Ni/alumina_850 catalyst in TGA SER multi-cycles. Reforming: 600 °C, steam/CH_4 = 4; regeneration: 850 °C, 8 min in 29/3/68 vol% steam/H_2/N_2.

weight change will be visible in the TGA. To assess the catalytic performance of the catalysts one needs to look at the kinetic curves.

The initial part of the kinetic curves as a function of cycle time (CC_t) along 100 SER/regeneration (29/3/68 vol% steam/H_2/N_2) cyclesfor the 15%Ni/alumina_850 catalyst and commercial catalyst is presented in Fig. 4. Sorbent saturation is reached within ~15 min for both samples (not presented in the graph). Since only CH_4 and steam were fed, and CO_2 sorption capacity was constant throughout 100 cycles (reported earlier [9]), the shift of the kinetics curves can be attributed to decrease of catalyst activity. It can be seen that shifting of kinetic curve is much more pronounced for the commercial catalyst compared to the 15%Ni/alumina_850 catalyst. This again, in accordance with the SMR test, indicates that catalyst calcined at high temperature (850 °C) is much more resistant towards sintering even under cycling conditions. This is robustness is due to the strong interaction of Ni with the support where the Ni migration is suppressed [36,40]. This is confirmed by the growth of Ni crystalline size after SER cycling. The Ni-crystallite size of the commercial catalyst increased from 15 to 30 nm while Ni crystallite size of 15%Ni/alumina_850 increased from 17 nm to 26.5 nm after SER 100 cycles. This is in accordance with the SMR stability test performed in the PBR (summarized in Table 4).

4. Conclusions

Series of 15%Ni/alumina catalysts have been synthesized and calcined at different temperatures (350–850 °C) and tested for hydrogen production in steam methane and sorption enhanced reforming. The catalyst calcined at highest temperature of 850 °C showed the highest CH_4 conversion and hydrogen production in steam methane reforming compared to the catalysts calcined at lower temperatures. In addition, the catalyst showed much better stability when exposed to the harsh conditions (high temperature and steam) compared to the catalysts calcined at lower temperatures and typical commercial reforming catalyst. Moreover, the catalyst calcined at 850 °C showed much better stability after 100 SER/regeneration cycles. This is due to the formation of the Ni aluminate during calcination which provides Ni fixation in the support and thus, higher resistance towards deactivation.

CRediT authorship contribution statement

L.J. Gavrilović: Conceptualization, Methodology, Writing – original draft. **S.S. Kazi:** Methodology, Data curation, Writing – review & editing. **A. Nelson:** Visualization, Methodology, Investigation. **A.G.P. Oliveira:** Conceptualization, Writing – review & editing. **J. Meyer:** Supervision, Writing – review & editing.

Declaration of Competing Interest

The authors declare the following financial interests/personal relationships which may be considered as potential competing interests.

Ljubisa Gavrilovic reports financial support was provided by Horizon 2020.

Data availability

No data was used for the research described in the article.

Acknowledgment

The presented work is funded within the CONVERGE project as part of the European Union's H2020 Research and Innovation Action project, Grant Agreement number 818135.

References

[1] International Energy Agency, Net Zero by 2050, 2021.
[2] L. di Felice, S.S. Kazi, M.H. Sørby, I. Martinez, G. Grasa, D. Maury, J. Meyer, Combined Sorbent and Catalyst Material for Sorption Enhanced Reforming of methane under Cyclic Regeneration in Presence of H2O and CO2, Fuel Process. Technol. 2019 (183) (October 2018) 35–47, https://doi.org/10.1016/j.fuproc.2018.10.012.
[3] I. Aloisi, A. di Giuliano, A. di Carlo, P.U. Foscolo, C. Courson, K. Gallucci, Sorption Enhanced Catalytic Steam methane Reforming: Experimental Data and Simulations describing the Behaviour of Bi-Functional Particles, Chem. Eng. J. 314 (2017) 570–582, https://doi.org/10.1016/j.cej.2016.12.014.
[4] A. Di Giuliano, K. Gallucci, S.S. Kazi, F. Giancaterino, A. Di Carlo, C. Courson, J. Meyer, L. Di Felice, Development of Ni- and CaO-Based Mono- and Bi-Functional Catalyst and Sorbent Materials for Sorption Enhanced Steam methane Reforming: Performance over 200 Cycles and Attrition Tests, Fuel Process. Technol. (2019) 195, https://doi.org/10.1016/j.fuproc.2019.106160.
[5] S.K. Bhatia, D.D. Perlmutter, Effect of the Product Layer on the Kinetics of the CO2-Lime Reaction, AICHE J. 29 (1) (1983), https://doi.org/10.1002/aic.690290111.
[6] B. Feng, W. Liu, X. Li, H. An, Overcoming the Problem of Loss-in-Capacity of Calcium Oxide in CO 2 Capture, Energy Fuel 20 (6) (2006), https://doi.org/10.1021/ef060258w.
[7] G.S. Grasa, J.C. Abanades, CO 2 Capture Capacity of CaO in Long Series of Carbonation/Calcination Cycles, Ind. Eng. Chem. Res. (2006) 45 (26), https://doi.org/10.1021/ie0606946.
[8] J. Mastin, A. Aranda, J. Meyer, New Synthesis Method for CaO-Based Synthetic Sorbents with Enhanced Properties for High-Temperature CO2-Capture, Energy Procedia 4 (2011) 1184–1191, https://doi.org/10.1016/j.egypro.2011.01.172.
[9] S.S. Kazi, A. Aranda, J. Meyer, J. Mastin, High Performance CaO-Based Sorbents for Pre- and Postcombustion CO2 Capture at High Temperature, Energy Procedia 2014 (63) (1876) 2207–2215, https://doi.org/10.1016/j.egypro.2014.11.240.
[10] J. Meyer, J. Mastin, C.S. Pinilla, Sustainable Hydrogen Production from Biogas using Sorption- Enhanced Reforming, Energy Procedia 2014 (63) (1876) 6800–6814, https://doi.org/10.1016/j.egypro.2014.11.714.
[11] A.L. García-Lario, M. Aznar, I. Martinez, G.S. Grasa, R. Murillo, Experimental Study of the Application of a NiO/NiAl2O4 Catalyst and a CaO-Based Synthetic Sorbent on the Sorption Enhanced Reforming Process, Int. J. Hydrog. Energy 40 (1) (2015) 219–232, https://doi.org/10.1016/j.ijhydene.2014.10.033.
[12] H.K. Rusten, E. Ochoa-Fernández, H. Lindborg, D. Chen, H.A. Jakobsen, Hydrogen Production by Sorption-Enhanced Steam methane Reforming using Lithium Oxides as CO2-Acceptor, in: Industrial and Engineering Chemistry Research vol. 46, American Chemical Society, 2007, pp. 8729–8737, https://doi.org/10.1021/ie070770k.
[13] J. Phromprasit, J. Powell, S. Wongsakulphasatch, W. Kiatkittipong, P. Bumroongsakulsawat, S. Assabumrungrat, H2 production from Sorption Enhanced Steam Reforming of Biogas using Multifunctional Catalysts of Ni over Zr-, Ce- and La-Modified CaO Sorbents, Chem. Eng. J. 313 (2017) 1415–1425, https://doi.org/10.1016/j.cej.2016.11.051.
[14] B. Arstad, J. Prostak, R. Blom, Continuous Hydrogen Production by Sorption Enhanced Steam methane Reforming (SE-SMR) in a Circulating Fluidized Bed Reactor: Sorbent to Catalyst Ratio Dependencies, Chem. Eng. J. 189–190 (2012) 413–421, https://doi.org/10.1016/j.cej.2012.02.057.
[15] J. Sehested, Sintering of Nickel Steam-Reforming Catalysts, J. Catal. 217 (2) (2003) 417–426, https://doi.org/10.1016/S0021-9517(03)00075-7.
[16] I. Martínez, G. Grasa, J. Meyer, L. di Felice, S. Kazi, C. Sanz, D. Maury, C. Voisin, Performance and Operating Limits of a Sorbent-Catalyst System for Sorption-Enhanced Reforming (SER)in a Fluidized Bed Reactor, Chem. Eng. Sci. 205 (2019) 94–105, https://doi.org/10.1016/j.ces.2019.04.029.

[17] Chang Jun Liu, Jingyun Ye, Y.P. Jiaojun Jiang, Progresses in the Preparation of Coke Resistant Ni-based Catalyst for Steam and CO 2 Reforming of methane, ChemCatChem 3 (3) (2011) 529–541.
[18] M.M. Yung, J.N. Kuhn, Deactivation Mechanisms of Ni-based Tar Reforming Catalysts as Monitored by X-Ray Absorption Spectroscopy, Langmuir 26 (21) (2010) 16589–16594, https://doi.org/10.1021/la1016593.
[19] B.C. Enger, R. Lødeng, J. Walmsley, A. Holmen, Inactive Aluminate Spinels as Precursors for Design of CPO and Reforming Catalysts, Appl. Catal. A Gen. 383 (1–2) (2010) 119–127, https://doi.org/10.1016/j.apcata.2010.05.033.
[20] N. Salhi, A. Boulahouache, C. Petit, A. Kiennemann, C. Rabia, Steam Reforming of methane to Syngas over NiAl2O4 Spinel Catalysts, Int. J. Hydrog. Energy 36 (17) (2011) 11433–11439, https://doi.org/10.1016/j.ijhydene.2010.11.071.
[21] X.L. Cai, G.Y. Li, W.M. Lin, Effect of Calcined Temperature on Coke Deposition for Autothermal Reforming of methane with Ni-Cu Catalyst, Chin. J. Chem. Phys. 28 (2) (2015) 217–222, https://doi.org/10.1063/1674-0068/28/cjcp1411195.
[22] J. Du, J. Gao, F. Gu, J. Zhuang, B. Lu, L. Jia, G. Xu, Q. Liu, F. Su, A strategy to Regenerate Coked and Sintered Ni/Al2O3 Catalyst for Methanation Reaction, Int. J. Hydrog. Energy 43 (45) (2018) 20661–20670, https://doi.org/10.1016/j.ijhydene.2018.09.128.
[23] S. Katheria, A. Gupta, G. Deo, D. Kunzru, Effect of Calcination Temperature on Stability and activity of Ni/MgAl2O4 Catalyst for Steam Reforming of methane at High pressure Condition, Int. J. Hydrog. Energy 41 (32) (2016) 14123–14132, https://doi.org/10.1016/j.ijhydene.2016.05.109.
[24] Y. Bae, J. Hong, Enhancement of Surface Morphology and Catalytic Kinetics of NiAl2O4 Spinel-Derived Ni Catalyst to Promote Dry Reforming of methane at Low Temperature for the Direct Application to a Solid Oxide fuel Cell, Chem. Eng. J. 446 (2022), 136978, https://doi.org/10.1016/j.cej.2022.136978.
[25] Y. Wang, D. Liang, C. Wang, M. Chen, Z. Tang, J. Hu, Z. Yang, H. Zhang, J. Wang, S. Liu, Influence of Calcination Temperature of Ni/Attapulgite on Hydrogen Production by Steam Reforming Ethanol, Renew. Energy 160 (2020) 597–611, https://doi.org/10.1016/j.renene.2020.06.126.
[26] S. Iglesias-Vázquez, J. Valecillos, A. Remiro, J. Bilbao, A.G. Gayubo, Stability of a NiAl2O4 Derived Catalyst in the Ethanol Steam Reforming in Reaction-Regeneration Cycles: effect of Reduction Temperature, Catalysts 12 (5) (2022) 550, https://doi.org/10.3390/catal12050550.
[27] A. Arandia, A. Remiro, V. García, P. Castaño, J. Bilbao, A. Gayubo, Oxidative Steam Reforming of Raw Bio-Oil over Supported and Bulk Ni Catalysts for Hydrogen Production, Catalysts 8 (8) (2018) 322, https://doi.org/10.3390/catal8080322.
[28] A. Remiro, A. Arandia, L. Oar-Arteta, J. Bilbao, A.G. Gayubo, Regeneration of NiAl2O4 Spinel Type Catalysts used in the Reforming of Raw Bio-Oil, Appl. Catal. B 237 (2018) 353–365, https://doi.org/10.1016/j.apcatb.2018.06.005.
[29] J.G. Seo, M.H. Youn, S. Park, J.S. Chung, I.K. Song, Hydrogen Production by Steam Reforming of Liquefied Natural Gas (LNG) over Ni/Al2O3–ZrO2 Xerogel Catalysts: effect of Calcination Temperature of Al2O3–ZrO2 Xerogel Supports, Int. J. Hydrog. Energy 34 (9) (2009) 3755–3763, https://doi.org/10.1016/j.ijhydene.2009.03.030.
[30] S. Kazi, G.N. Kalantzopoulos, S.S. Kazi, G. Grasa, J. Mastin, R. Murillo, J. Meyer, Development of High Performance CO2 Solid Sorbents Combined with a Reforming Catalyst for Hydrogen Production by Sorption-Enhanced Reforming (SER) Development of High Performance CO 2 Solid Sorbents Combined with a Reforming Catalyst for Hydrogen Production by Sorption-Enhanced Reforming (SER). https://www.researchgate.net/publication/277015150, 2017.
[31] R. López-Fonseca, C. Jiménez-González, B. De Rivas, J.I. Gutiérrez-Ortiz, Partial Oxidation of methane to Syngas on Bulk NiAl 2O 4 Catalyst. Comparison with Alumina Supported Nickel, platinum and Rhodium Catalysts, Appl. Catal. A Gen. (2012), https://doi.org/10.1016/j.apcata.2012.06.014, 437–438, 53–62.
[32] Y. Echegoyen, I. Suelves, M.J. Lázaro, R. Moliner, J.M. Palacios, Hydrogen Production by Thermocatalytic Decomposition of methane over Ni-Al and Ni-Cu-Al Catalysts: effect of Calcination Temperature, J. Power Sources 169 (1) (2007) 150–157, https://doi.org/10.1016/j.jpowsour.2007.01.058.
[33] Y. Ding, C. Zhao, Y. Li, Z. Ma, X. Lv, Effect of Calcination Temperature on the Structure and Catalytic Performance of the Cu-Mcm-41 Catalysts for the Synthesis of Dimethyl Carbonate, Quim Nova 41 (10) (2018) 1156–1161, https://doi.org/10.21577/0100-4042.20170291.
[34] C. Jiménez-González, Z. Boukha, B. De Rivas, J.J. Delgado, M.Á. Cauqui, J. R. González-Velasco, J.I. Gutiérrez-Ortiz, R. López-Fonseca, Structural Characterisation of Ni/Alumina Reforming Catalysts Activated at High Temperatures, Appl. Catal. A Gen. 466 (2013) 9–20, https://doi.org/10.1016/j.apcata.2013.06.017.
[35] M. Zangouei, A.Z. Moghaddam, M. Arasteh, The Influence of Nickel Loading on Reducibility of NiO/Al_2O_3 Catalysts Synthesized by Sol-Gel Method, Chem. Eng. Res. Bull. 14 (2) (2010) 97–102, https://doi.org/10.3329/cerb.v14i2.5052.
[36] L. Zhou, L. Li, N. Wei, J. Li, J.M. Basset, Effect of NiAl2O4 Formation on Ni/Al2O3 Stability during Dry Reforming of methane, ChemCatChem 7 (16) (2015) 2508–2516, https://doi.org/10.1002/cctc.201500379.
[37] A. Chatla, M.M. Ghouri, O.W. el Hassan, N. Mohamed, A.V. Prakash, N.O. Elbashir, An Experimental and first Principles DFT Investigation on the effect of Cu Addition to Ni/Al2O3 Catalyst for the Dry Reforming of methane, Appl. Catal. A Gen. 602 (2020), 117699, https://doi.org/10.1016/j.apcata.2020.117699.
[38] B.C. Enger, R. Lødeng, J. Walmsley, A. Holmen, Inactive Aluminate Spinels as Precursors for Design of CPO and Reforming Catalysts, Appl. Catal. A Gen. 383 (1–2) (2010) 119–127, https://doi.org/10.1016/j.apcata.2010.05.033.
[39] A. Al-Ubaid, E.E. Wolf, Steam Reforming of methane on Reduced Non-Stoichiometric Nickel Aluminate Catalysts, Appl. Catal. 40 (1988) 73–85, https://doi.org/10.1016/S0166-9834(00)80427-3.
[40] I. Czekaj, F. Loviat, F. Raimondi, J. Wambach, S. Biollaz, A. Wokaun, Characterization of Surface Processes at the Ni-based Catalyst during the Methanation of Biomass-Derived Synthesis Gas: X-Ray Photoelectron Spectroscopy (XPS), Appl. Catal. A Gen. 329 (2007) 68–78, https://doi.org/10.1016/j.apcata.2007.06.027.